

THE FOM-MEQALAC SYSTEM: LOW ENERGY BEAM TRANSPORT

F. Siebenlist, R.W. Thomae, P.W. van Amersfoort, E.H.A. Granneman  
FOM-Institute for Atomic and Molecular Physics,  
Kruislaan 407, 1098 SJ Amsterdam, The Netherlands

H. Klein, A. Schempp, T. Weis  
Institut für Angewandte Physik, University Frankfurt  
Robert-Mayerstrasse 2-4, 6000 Frankfurt/M, FRG

Summary

In MEQALAC systems a large number of small parallel beamlets is accelerated simultaneously. (Meqalac Electrostatic Quadrupole Array Linear Accelerator<sup>1</sup>.) In the first stage of the FOM-MEQALAC project four 40 keV He<sup>+</sup> beams are to be accelerated to 115 keV. The low energy beam transport section (LEBT) transports the four 40 keV beams from the ion source to the RF-accelerator. It consists of four parallel transport channels each made up of 34 electrostatic quadrupole singlet lenses. The first five quads are excited independently to match the cylindrically symmetric beams extracted from the source to the periodic focusing system of the rest of the LEBT and the MEQALAC section. The ion source and LEBT section are discussed. Measurements on the beam matching section are presented as well as calculations on the transport of space charge loaded beams through the quadrupole channel. Information on the RF accelerator is presented in an accompanying paper by Thomae et al.<sup>2</sup>.

Introduction

At low particle energies (<50 keV/N) the space charge loading of the beam sets severe limits to the current that can be transported and accelerated. A possible way to overcome this problem is to transport and accelerate, instead of a single beam, a large number of small parallel beamlets. The radial stability of each beamlet can be ensured by the use of periodic transverse focusing elements.

The MEQALAC system features the simultaneous acceleration of multiple parallel beamlets, while strong focusing electrostatic quadrupoles in between the acceleration gaps prevent space charge induced blow-up of the beams and counteract the radial defocusing effect of the acceleration gaps. The advantage of such a system is that in principle an arbitrarily large current can be accelerated by increasing the number of beamlets.

The LEBT section has the same transverse focusing grid as is present in the MEQALAC accelerator. So knowledge of the behaviour of the space charge loaded beams in this periodic focusing transport section is crucial for the understanding of the radial transport in the RF accelerator.

Experimental set-up

A schematic picture of the FOM-experiment is shown in figure 1. From a bucket type plasma source four He<sup>+</sup> beams are extracted. A low energy beam transport section (LEBT) transports the ions from the high pressure ion source region to the low pressure RF acceleration region. The first five lenses can be tuned individually to match the cylindrically symmetric beams coming out of the source to the periodic focusing systems of the LEBT and MEQALAC sections. Halfway the LEBT section the DC beams are bunched by means of a two-gap buncher and subsequently injected into the MEQALAC accelerator<sup>3,4,5</sup>.

The ion source

The source is a bucket type plasma source (see fig. 2), which has a diameter of 14 cm and a depth of 11 cm. On the outside of the source rings of CoSm magnets are mounted, giving a line cusp magnetic field, which reduces the plasma losses to the walls. The source front plate is insulated from the rest of the source and has

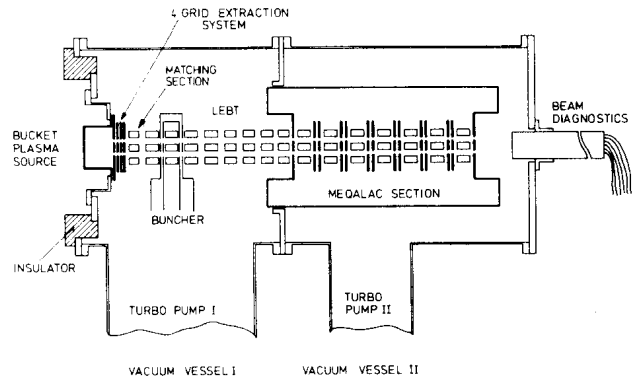


Fig. 1. The experimental set-up. For details see text.

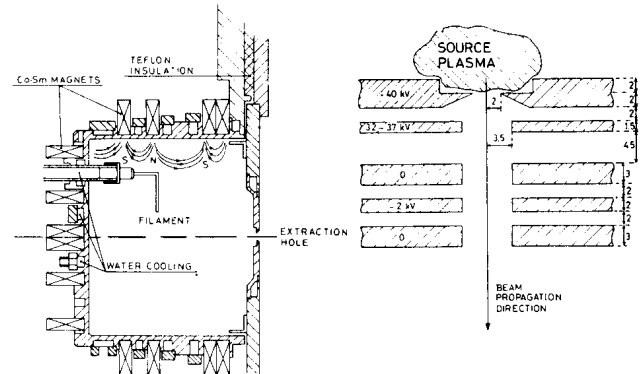


Fig. 2. The plasma source and the 40 kV extraction system. All dimensions are in mm. For details see text.

the same potential as the filaments. The two filaments are situated at the backwall of the source; one is used to generate the discharge. Four extraction apertures, of which the diameter can be chosen between 4 and 7 mm, are situated in the frontplate. In the present study 5.2 mm apertures are used.

The 40 kV extraction system (see fig. 2) is a modified version of the four-grid system described by Holmes<sup>6</sup>. By varying the second intermediate electrode (between 32 - 37 kV) the shape of the emittance diagrams can be changed. The duty cycle of the extraction system can be varied between 1% and 100%.

Typical operating parameters are: 40 kV extraction voltage, 10 mA/beamlet, 120 V arc voltage, 15 A arc current and a gas pressure in the source of  $8 \cdot 10^{-3}$  mbarr. The emittances of the extracted beams do not vary much with extracted current (6 - 14 mA) or with the potential on the intermediate electrode (4 - 8 kV with respect to the source body). It was consistently found to lie in the range 15 - 30  $\pi$ . mm. mrad (RMS values).

The LEBT section

A schematic view of the mounting of the quadrupole elements and the characteristic dimensions are shown in fig. 3 and 4. For 40 keV He<sup>+</sup> beams to be transported

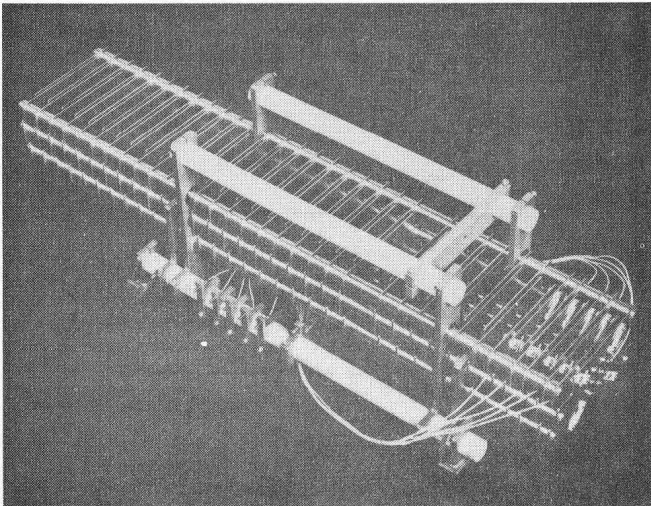


Fig. 3. Part of the low energy beam transport section.

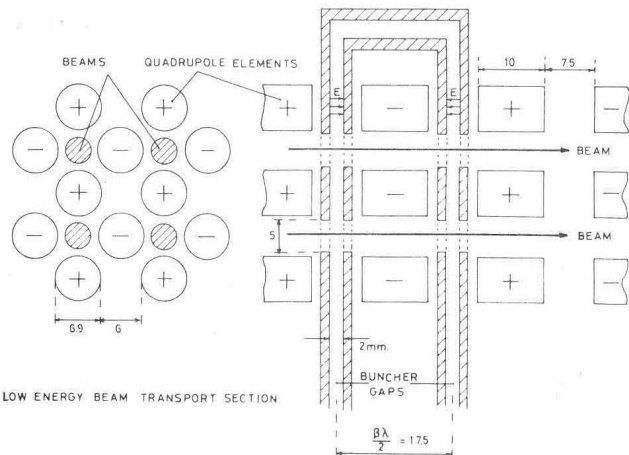


Fig. 4. Characteristic dimensions (in mm) of the LEBT section. Also the two-gap buncher is shown.

through this periodic focusing system, with  $\mu_0 = 60^\circ$ , quadrupole voltages of  $\pm 2.62$  kV are needed ( $\mu_0$ : phase advance per cell for zero current). For typical beam emittances of 15 and  $30 \pi \cdot \text{mm} \cdot \text{mrad}$  and a maximum filling factor of 5/6 (maximum beam radius = 2.5 mm) the theoretical space charge limited current is 19 and 18 mA ( $\mu = 8.3^\circ$  and  $16.6^\circ$  resp.)<sup>7</sup>.

The first quadrupole lens element is situated 18.7 mm behind the last grid of the source extraction system. The four gaps between the first five quads (the matching section) are 3, 3, 5 and 5 mm, respectively.

Beam diagnostics

The total current of the four beams is measured with a Faraday cup.

The envelope (E), its derivative (E') and the emittance ( $\epsilon$ ) of an individual beamlet are measured with an emittance measuring device. This device consists of a movable entrance slit and an array of 40 parallel wires. The whole device can be rotated to measure the emittance diagram of the x-plane as well as the y-plane. An example of such emittance diagrams is given in fig.5.

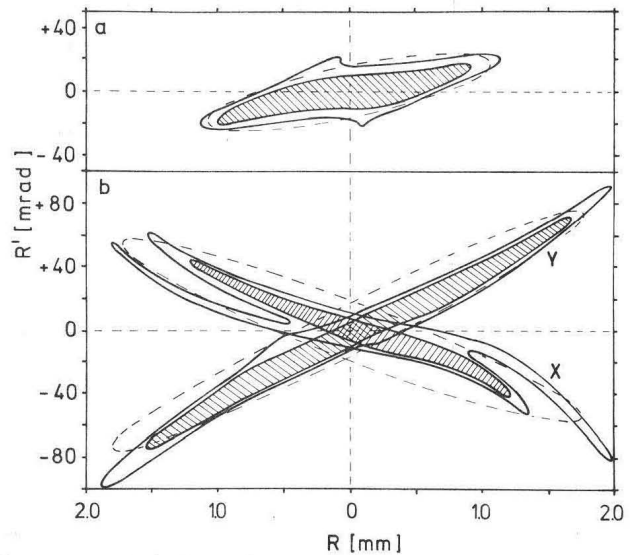


Fig. 5. Emittance diagrams. The outer solid lines indicate the contours where the intensity is 10% of the maximum value. The solid lines enclosing the shaded area represent the 36.8% (1/e) contours. The dashed lines give the RMS ellipses as deduced from the measured intensity distribution.

- 5a. Emittance diagrams of a 14 mA beam at the entrance plane of the first quadrupole:  $E_x = E_y = 1.08$  mm;  $E'_x = E'_y = 17.9$  mrad;  $\epsilon = 17.6 \pi \cdot \text{mm} \cdot \text{mrad}$  (RMS values);  $\epsilon(1/e) = 8.5 \pi \cdot \text{mm} \cdot \text{mrad}$ .
- 5b. Emittance diagram of the beam x and y planes, measured behind the sixth quadrupole. The orientation of the diagrams is equal to the calculated ones within 15%. The x and y diagrams are not fully symmetric because the actual slit is 2 mm behind the grounded front plane of the emittance measuring device. This grounded front plate is placed at the centre of the gap separating two successive quadrupoles.  $E_x = 1.75$  mm,  $E'_x = -54$  mrad,  $\epsilon_x = 32 \pi \cdot \text{mm} \cdot \text{mrad}$ ,  $E_y = 1.79$  mm,  $E'_y = 74$  mrad,  $\epsilon_y = 30 \pi \cdot \text{mm} \cdot \text{mrad}$  (all RMS values);  $\epsilon_x(1/e) = 8.0 \pi \cdot \text{mm} \cdot \text{mrad}$ ,  $\epsilon_y = 12.4 \pi \cdot \text{mm} \cdot \text{mrad}$ .

Calculations and measurements

For the radial matching of the beams extracted from the ion source to the periodic solution of the second part of the LEBT section and the MEQALAC accelerator a computer code was developed based on the so-called Kapchinsky-Vladimirsky (KV) equations<sup>8,9</sup>. This is a set of two coupled equations which can be used to calculate the transport of space charge loaded beams through quadrupole transport systems. The code first calculates the periodic solution of the transport section for the extracted beam current and emittance. Subsequently it calculates the voltages with which the first five quadrupoles must be excited in order to match the beam entering the first quadrupole (with characteristic parameters: envelope  $E_x = E_y = E$ , envelope derivative  $E'_x = E'_y = E'$  and emittance  $\epsilon_x = \epsilon_y = \epsilon$ ) to the periodic solution of the rest of the LEBT. Halfway two quadrupoles this solution is characterized by  $E_x = E_y$ ,  $E'_x = -E'_y$ . At present the model assumes hard-edge quadrupole fields, i.e. the field is constant from the entrance to the exit plane of the quad and zero in between quads. This model is probably too simple. It was found that it was not able to predict the beam behaviour for all injected beams correctly. A more sophisticated field model, developed at LBL<sup>10</sup>, which takes fringe fields properly into account, is presently being incorporated.

Results of the hard-edge model are shown in fig. 6 for a 14 mA beam. The entrance parameters are based on



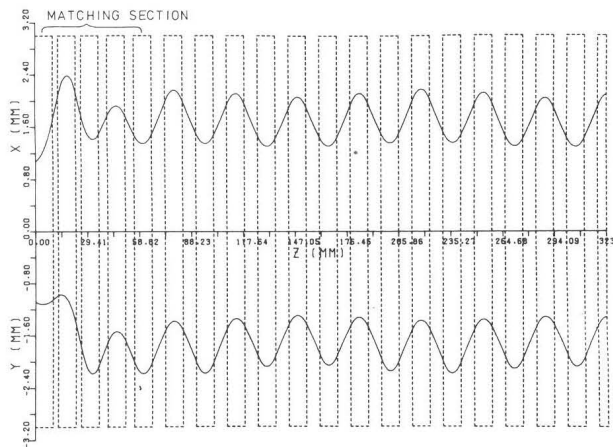


Fig. 6. KV beam envelope calculations for the first 20 quads of the LEBT section. In the top and bottom half of the picture the envelopes in the x and y planes, respectively, are shown. The 14 mA beam of fig. 5a is injected. The voltages on the first five (matching section) quads are: 2.10 kV, 3.91 kV, 3.57 kV, 2.57 kV, 2.57 kV. The voltage on the rest of the LEBT quads is 2.62 kV.

the RMS-values deduced from measurements done at the entrance plane of the first quadrupole (figure 5a). Measurements were also done with the grounded frontplate of the emittance measuring device placed at a distance of 3.75 mm behind the sixth quadrupole, i.e. at a location where the periodic solution is valid. The values for the 14 mA beam are shown in fig. 5b for the x and y planes. The transmission of this part of the system was found to be 95%.

Two conclusions can be drawn from the measurements of fig. 5. First, for this particular case the hard-edge model yields voltages for the matching section quads resulting in emittance diagrams with approximately correct ( $\sim 15\%$ ) values for  $E_x$ ,  $E_y$ ,  $E_x'$  and  $E_y'$ . Secondly, large aberrations have developed during transport in the first six lenses, especially in the x-plane. Furthermore the RMS emittance of the beam has increased considerably in both planes (the  $1/e$  emittance has increased appreciably only in the y-plane). The reason for the emittance growth and the development of aberrations is not yet fully understood. Both effects may be caused by the fact that the emittance diagram of the injected beam already shows some aberrations. A second cause may be that hard-edge quadrupoles have relatively strong non-linear fringe fields. Thirdly, possibly the filling of the channel is too large, causing further non-linearities. All these effects will be studied more carefully in the near future.

#### References

1. A.W. Maschke, Brookhaven Natl.Lab., report BNL-51209 (1979).
2. R.W. Thomae, F. Siebenlist, P.W. van Amersfoort, E.H.A. Granneman, H. Klein, A. Schempp, T. Weis, these proceedings.
3. P.W. van Amersfoort, E.H.A. Granneman, J. Kistemaker, F. Siebenlist, R.W. Thomae, H. Klein, A. Schempp, FOM-report nr. 55.120, November 1982.
4. F. Siebenlist, R.W. Thomae, P.W. van Amersfoort, E.H.A. Granneman, J. Kistemaker, H. Klein, A. Schempp, FOM-report nr. 56.298, May 1983.
5. R.W. Thomae, P.W. van Amersfoort, F. Siebenlist, F.G. Schonewille, E.H.A. Granneman, J. Kistemaker, H. Klein, A. Schempp, T. Weis, FOM-report nr. 57.379, December 1983.
6. A.J.T. Holmes, E. Thompson, F. Watters, J.Phys. E14, 856 (1981).

7. M. Reiser, Part.Acc. 8, 167 (1978); J.Appl.Phys. 52, 555 (1981).
8. I.M. Kapchinsky, V.V. Vladimirski, Proc.Int.Conf.on High Energy Acc., CERN, Geneva, 1959, page 274.
9. F.J. Sacherer, IEEE Trans.Nucl.Sci. NS18, 1105 (1971).
10. L.J. Laslett, D. Keefe, C.H. Kimm, M. Tiefenback, A.I. Warwick, private communication, LBL, 1984.

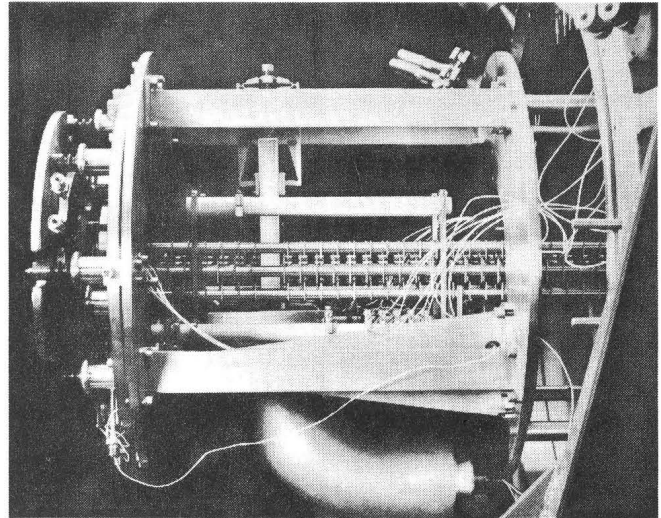


Fig. 7. The LEBT section. The 40 kV extraction system is mounted on the left side of the support which also holds the quadrupole lens elements. The buncher with the (90° bended) coaxial pipe and the capacitive tuning mechanism is seen in the middle.